

# Case Study: Seismic Stability of Underwater Retaining Walls

Mark Sinclair: Maunsell Ltd, Auckland, New Zealand

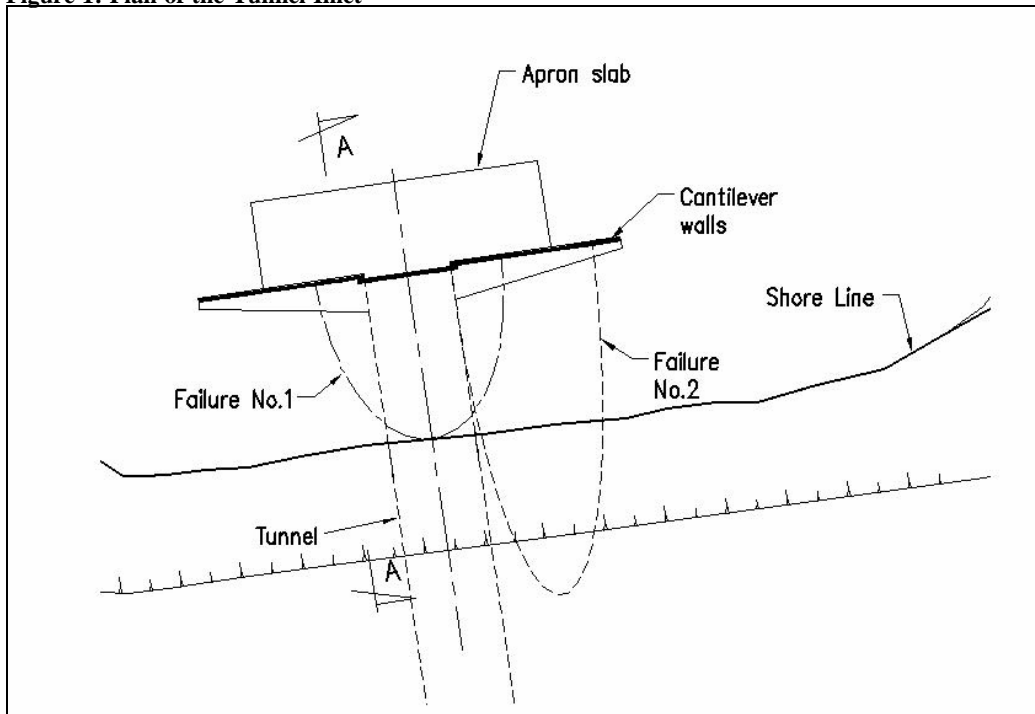
The upstream end of a reservoir's outlet structure is retained by 9 to 12m high retaining walls. The effect on retaining wall stability of a 3 to 4m thick layer of gravels deposited upslope of the walls, particularly retaining wall stability under seismic loading, has been assessed.

This paper details the method of stability analysis, modelling three-dimensional effects of the reservoir shoreline slope and wall geometries, modelling wall reactions, soil and hydrodynamic loads, and determination of seismic displacements. Different thicknesses of deposited surcharge material were modelled, as were different reservoir levels. Both drained and undrained conditions on the failure surface under earthquake loading were considered. Results are presented for stability, sensitivity, wall capacity and shoreline slope displacement.

## 1.0 Background

The upstream end of a reservoir's outlet structure is retained by 9 to 12m high retaining walls. Figure 1 below shows a plan of the outlet structure and location of the retaining walls.

**Figure 1: Plan of the Tunnel Inlet**



A review report recommended an updated assessment of retaining wall stability for the latest seismic hazard information and wall surcharge loadings. This assessment comprised assessing wall displacements required for first cracking, first yield and ultimate capacities and comparing wall displacements to slope displacements, which were assessed from three earthquake records using the Newmark Sliding Block Method. Further assessments were recommended comprising a more detailed assessment of the structural performance of the walls, and consideration of the three dimensional effects of the vent shaft, and apron on the shoreline slope failure geometry. The potential for tunnel blockage was also to be assessed.

This paper details the method of stability analysis, modelling three dimensional effects of the slope and wall geometries, modelling wall reactions, soil and hydrodynamic loads, and determination of seismic displacements.

Seismic performance of the walls was initially assessed by a force based approach, which computed earth pressures on the back of the walls for various failure geometries and compared earth pressures with wall structural capacities. Seismic earth pressures were determined using the Monobe Okabe equation. However this equation was not appropriate for the slope geometry and higher seismic coefficients, and a graphical approach (Culmann's method) was then used to calculate earth pressures on the back of the wall. The force based approach indicated that wall capacities were exceeded for relatively low return period earthquakes (about 150 years).

A displacement based approach was then considered as this approach recognises that:

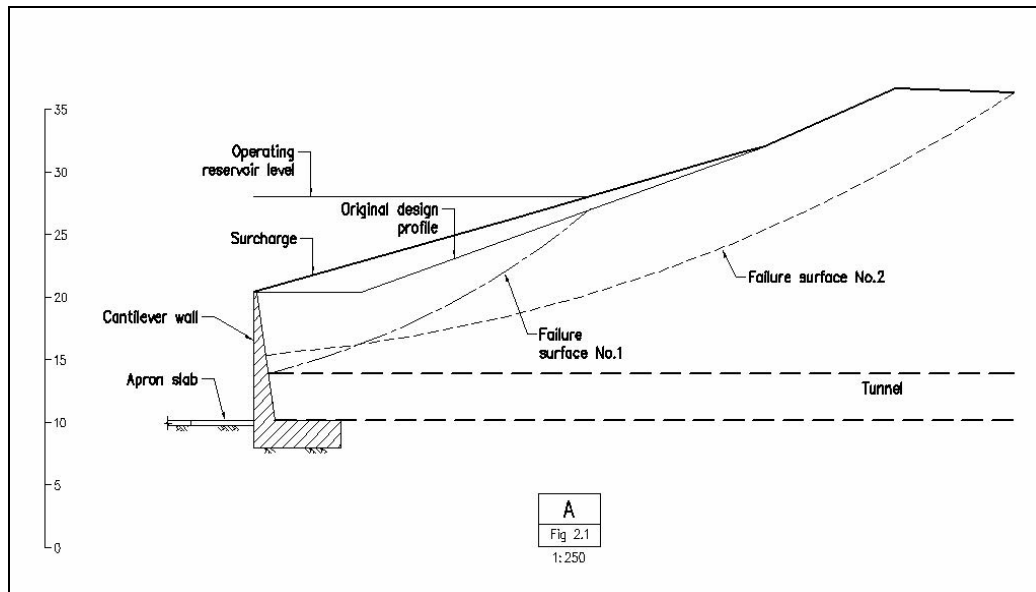
- a) the mobilised wall resistance is dependant on wall displacements
- b) the shoreline slope will displace a finite amount for the earthquake considered and not necessarily experience catastrophic failure.

Slope displacements are then compared with wall capacity displacements to determine the condition of the wall (i.e. first cracking, yield or ultimate capacity). This approach assumes that shoreline slope displacement will cause a similar displacement in the walls.

## 2.0 Wall, Shoreline Slope and Failure Surface Geometries

As-built drawings were used to define wall and slope geometries. Figure 2 shows a section (A-A) through the cantilever wall and slope.

**Figure 2: Section A-A Through Cantilever Wall and Slope**



The cantilever walls are restrained above their base by the apron slab, wall foundation embedment and slope. Wall displacement by rotation and sliding at foundation level is therefore prevented and the wall section above the level of the apron slab contact resists static and seismic loads. The counterfort wall and the upstream section of the tunnel are monolithic. The apron slab and shear key embedment at the upstream end of the tunnel prevent sliding of the tunnel and wall. Wall displacement by rotation and sliding at tunnel foundation level is therefore prevented and the counterfort section at the top of the tunnel and panels between counterforts resist static and seismic loads.

Two failure surfaces in the shoreline slope were used to partially model the three-dimensional effects of the slope and wall geometries and the vent shaft on shoreline slope failure. Figures 1 and 2 show the

location of the assumed failure surfaces. Failure No.1 was located behind the wall and constrained to mid slope with the maximum depth limited by the top of the tunnel. Failure No.2 (critical surface) was located behind the walls between the tunnel and abutments and extended to the top of the slope. The maximum depth of failure No.2 at the cantilever walls was limited by the sloping apron slab and represents a reasonable maximum depth for a three-dimensional failure surface behind the cantilever walls.

The computer program Slope/W was used to determine failure surface geometries given the above boundary constraints. Slope/W models the failure surface in a two-dimensional plane and published research suggests that factors of safety computed for a three-dimensional surface are always higher due to the restraining effects of the shear forces on the sides and ends of the sliding mass. Hence the factors of safety determined for failure surfaces No.1 and 2 are conservative.

### **3.0 Wall Structural Assessment**

For the cantilever walls the critical section was defined as the part of the wall where fixity is assumed and the wall section can develop its ultimate strength. An equivalent wall reaction and location could then be determined. Two possible application points for the wall reactions were proposed. These were at the point where the average wall capacity was assessed which reflected the wall reaction pressure distribution at the wall base, and at 2/3 the depth of the failure surface from the top of the wall, which reflected the pressure distribution at the base of the failure surface.

Wall capacity displacements were then determined corresponding to first cracking, first yield and ultimate capacity (reinforcing steel tensile failure). A permissible wall crack width was used to define wall serviceability. Displacements midway between top of wall and the failure surface were used for comparing slope displacement and hence wall performance.

### **4.0 Upstream Shoulder Displacements**

Seismic induced displacements of the slope were calculated using the Newmark method of double integration. This involved determining minimum factors of safety (static) and critical accelerations (earthquake pseudo static) for the two failure surfaces using Slope/W software and using the critical accelerations with earthquake time histories to determine slope displacements.

The Slope/W wall reactions and Newmark displacement analysis were iterated for each of the 150, 1,000 and 10,000 year earthquake records until the shoulder (seismic induced) displacement matched the wall displacement (established from structural assessment) for the Slope/W wall reaction used.

Four earthquake acceleration time history records from overseas were used since suitable local records are not available. These were:

- Valparaiso, Chile (Richter magnitude 7.4)
- Vile, Mexico (Richter magnitude 8.1)
- Landers, USA (Richter magnitude 7.0)
- Tabas, Iran (Richter magnitude 7.0)

The Chile, Mexico and Iran records were scaled to give peak ground accelerations for the site spectra 150, 1,000 and 10,000 year return period events, i.e. 0.2g, 0.39g and 0.75g respectively. The USA record represents the expected record from an earthquake on a nearby fault which contributes a significant portion of the total seismic risk at the tunnel location.

The displacement calculation included reversal of earthquakes, and upslope movement was not permitted.

## 5.0 Slope Stability Assessment

### 5.1 Load Cases

For each of the two slope failure surfaces, three slope geometries were considered to account for the varying levels of deposited surcharge material. These were the “No Surcharge” construction as-built case, the “Surcharge” case, and the “Intermediate Surcharge” case.

Three reservoir levels were also considered for the slope stability model. These were, low reservoir level, operating reservoir level, and high reservoir level. For each reservoir level, seismic hydrodynamic effects on the retaining walls and the slope were considered.

Density and strength parameters of the slope and surcharge material were obtained from the design records. For the slope stability model, three values for the effective friction angle for the slope material were considered. Slope and surcharge material parameters are presented in Table 5.1 below.

**Table 5.1 Material strength parameters considered for stability model**

Slope material			Surcharge material		
Density (saturated) (kN/m <sup>3</sup> )	Effective cohesion (kPa)	Effective friction angle (degrees)	Density (saturated) (kN/m <sup>3</sup> )	Effective cohesion (kPa)	Effective friction angle (degrees)
23	0	36, 38 and 40	18	0	28

### 5.2 Wall Reactions

The wall reactions for the cantilever and counterfort walls were modelled as horizontal line loads applied just inside the vertical face (i.e. inside the sliding mass) at the toe of the slope.

### 5.3 Modelling of Reservoir

When modelling a structure such as an underwater slope, problems can arise in stability calculations when the failure surface is partially submerged or in the case here for failure surface 1, completely submerged. For the case with failure surface 1 where the failure mass is completely submerged, the reservoir was modelled as a no strength layer and a piezometric line along to the reservoir surface was applied. A second analysis was then run which did not include the reservoir as a layer or include a piezometric surface, but modelled the slope and surcharge material unit weights as a submerged unit weights. Very little discrepancy (0.2% difference) in factor of safety values between the two methods was found and the no strength soil layer method was adopted for the remaining analyses.

### 5.4 Drained and Undrained Parameters

Both drained and undrained conditions on the failure surface were considered. Slope/W allows for the modelling of undrained conditions with drained input parameters by using the failure surface shear resistance for the critical static drained failure surface and converting this to an equivalent  $\phi = 0^\circ$  shear resistance for the earthquake case.

### 5.5 Hydrodynamic Forces

Seismic hydrodynamic effects on walls and the slope were considered for each reservoir level. The hydrodynamic loads were applied as horizontal line loads applied at 2/3 wall height from the top of the walls and 2/3 the slope height below reservoir level. These hydrodynamic loads act in the opposite direction to wall reactions.

### 5.6 Sensitivity Analysis

Before selecting the critical load case for analysis a number of sensitivity analyses were carried out including varying the wall reaction application point, varying soil effective strength parameters, using drained and undrained parameters, and varying application point of hydrodynamic loads.

The sensitivity of Slope/W factors of safety to the level of application of the wall reaction line load was assessed. From the structural assessment of the walls two wall reaction locations were proposed. It was found that factors of safety were not significantly sensitive to the location of application of the line load and an average level of application was adopted.

Three effective stress friction angles for the slope material were considered ( $\phi'=36, 38$  and  $40^\circ$ ) and the sensitivity of these to displacements was assessed. It was found that displacements for the  $\phi'=38^\circ$  and  $40^\circ$  were 20% and 40% less than the corresponding  $36^\circ$  displacement. The typical level of confining stress (i.e. vertical effective stress at the failure surface for operational reservoir level and surcharge) is 140 kPa and documented research on triaxial tests on similar size range materials showed that a friction angle of  $40^\circ$  or more could be expected at confining pressures less than 140kPa. Hence an effective stress friction angle of  $40^\circ$  was adopted.

Displacements for drained and undrained failure surface conditions were assessed and displacements for the drained condition were found to be 60% to 90% greater than for the undrained case. It was felt that using drained conditions might not be appropriate due to the low-permeability material that the failure surface predominantly passes through, and the earthquake loading being rapid. Undrained conditions were hence adopted for analysis.

The sensitivity of the analysis to hydrodynamic loads was assessed. It was found that for hydrodynamic loads on walls and hydrodynamic loads on walls plus the slope component, factors of safety were not significantly sensitive. It was also felt that applying hydrodynamic loads to such a small area of reservoir was somewhat conservative and hence the “No hydrodynamic” case was adopted.

### 5.7 Critical Load Case for Analysis

The load case selected for slope displacement assessment for failures 1 and 2 was intermediate surcharge, operating reservoir level, no hydrodynamic load, and 150, 1,000 and 10,000 year events for all 4 seismic records. The intermediate surcharge geometry was selected as it represented a profile that could be readily maintained by dredging. Operating reservoir level was chosen as an “average” condition between high and low reservoir levels.

The two critical cases were then modelled with varying wall reactions and corresponding critical acceleration coefficients determined. The wall reactions and critical accelerations were used in the Newmark displacement analysis and iterated for each of the 150, 1,000 and 10,000 year earthquake records.

### 6.0 Wall Capacity and Slope Displacement Results

The following table compares wall capacity displacements with slope displacements for the walls.

**Table 6.0: Wall capacity and slope displacements**

Wall type	Wall capacity displacements (mm)				Slope displacements (mm)		
	First cracking	Yield	Ultimate	Serviceability	150 year event	1,000 year event	10,000 year event
Cantilever walls	3 to 4	15 to 26	70 to 195	15 to 28	0	0	7 to 47 Average 28

### 7.0 Conclusions

After reviewing the wall capacity displacements, slope displacements, and volume of displaced surcharge deposits, the following was concluded:

- Performance of the cantilever walls under the 150 and 1,000 year seismic events is satisfactory
- Displacements for cantilever walls may exceed the serviceability displacement (0.4mm crack width) under the 10,000 year event but will remain below ultimate (collapse) displacements
- The calculated slope displacements will not result in collapse of the cantilever walls nor will they contribute to a slope failure.
- Tunnel inlet blockage by seismic induced displacement of surcharge material is unlikely.